Solar-Terrestrial Physics. 2018. Vol. 4. Iss. 4. P. 82–87. DOI: 10.12737/stp-44201811. © 2018 S.V. Lesovoi, V.S. Kobets. Published by INFRA-M Academic Publishing House
Original Russian version: S.V. Lesovoi, V.S. Kobets, published in Solnechno-zemnaya fizika. 2018. Vol. 4. Iss. 4. P. 106–113. DOI: 10.12737/szf-44201811 © 2018 INFRA-M Academic Publishing House (Nauchno-Izdatelskii Tsentr INFRA-M)

SIMULATING SIBERIAN RADIOHELIOGRAPH RESPONSE TO THE QUIET SUN

S.V. Lesovoi
Institute of Solar-Terrestrial Physics, Irkutsk, Russia, svlesovoi@gmail.com

V.S. Kobets
Institute of Solar-Terrestrial Physics, Irkutsk, Russia, kobets@iszf.irk.ru

Abstract. The Siberian Radioheliograph (SRH) correlation plot is the time dependence of the sum of absolute values of complex correlations over all baselines. These plots are built for each operating frequency of SRH. The correlation is related not only to the spatial coherence of the incident microwave emission but also to antenna gains. That is why we have to consider real SRH antenna gains and shadowings. Correlation plots obtained by SRH are related to microwave flux density of the Sun and spatial features of microwave sources. Also the correlation plots show variability of SRH beam pattern in time with constant flux density and spatial structure of sources. The SRH beam pattern depends on position of the Sun with respect to SRH, which changes with time. This leads to variations of these plots, which can be confused, for example, with the quasi-harmonic oscillations of the microwave flux produced by sources located above sunspots. Because the solar disk is an extended source, the correlation plot variability is mostly due to the SRH response to the quiet Sun. The smaller is the microwave source, the smaller are the correlation plot variations caused by a change of the beam pattern. Relatively fast variations result from long baseline responses, so it is undesirable to exclude them from the plots. Moreover, the sensitivity of the plots is better when all baselines are taken in account. The impact of the correlation plot variations on the eruptive event response is especially strong because variations of microwave flux during such events are comparable with those of the correlation plots in magnitude and time. From the above it seems reasonable to simulate the SRH response to the quiet solar disk and correct the correlation plots.

In this work, we propose a method for simulating correlation plots, which allows us to correct their variations caused by time and frequency dependence of SRH response to the solar disk. The correlation plots are simulated either by summing all model antenna pair responses to the model solar disk or by summing the corresponding values of the solar disk visibility under the assumption that the visibility is $\sim J_1(x)/x$, where $J_1(x)$ is the Bessel function of the first kind. Also we consider the shadowing of antennas nearest to the center of the SRH antenna array.

Keywords: solar radio telescope, visibility function, correlation, radio interferometer.

INTRODUCTION

The study of low-energy solar events is important because of their large number, which allows more accurate identification of statistical regularities of solar activity. Furthermore, the total decrease in the solar activity level during the current cycle enables us to observe the events that are masked by more powerful events during periods of high solar activity. The interest in the low-energy events is due to the fact that, according to some assumptions, solar corona heating is caused by a large number of fairly continuously occurring weak solar flares [Parker, 1988; Knizhnik et al., 2018]. The question as to how weak are flares detected by observation of the solar microwave emission is therefore also of interest. In this paper, we analyze instrumental parameters of the multifrequency Siberian Radioheliograph (SRH) developed during modernization of the Siberian Solar Radio Telescope [Grechnev et al., 2003; Lesovoi et al., 2012, 2017]. The SRH data most sensitive to microwave emission flux density are the so-called correlation plots (CP) – the time dependence of the sum of absolute values of complex correlations over all baselines [Lesovoi, Kobets, 2017]. These plots are also convenient for the study of diurnal or day-to-day solar activity dynamics. The convenience is due to the data compactness and high sensitivity up to 0.01 s.f.u. However, CPs vary with time not only due to a change in the incident flux density. A change in CP may be caused by a change in the spatial structure of microwave sources or SRH beam pattern (BP). The CP temporal variations caused by a BP change may be non-monotonic and therefore can mask weak solar activity. The CP variations are most pronounced in the response to the solar disk, their level can reach 0.1 %, which corresponds to the emission flux density from 0.5 to 1.0 s.f.u. depending on the operating frequency. The level of the response from compact sources is generally a few percent, so the impact of CP variations on this response is negli-

gible. It is, however, necessary to correct the response for these variations when studying extremely weak solar activity. To correct the CP variations caused by a change in the response to the solar disk, we should subtract this response from the total response. An example of the CP variations is given in Figure 1. The "hills" marked with the oval on the two plots corresponding to high frequencies show up at other frequencies as more flat areas or areas with an overall long-term increase in the level of the response. Figure 2 illustrates how these variations occur during the year. The light arcs symmetric about the noon indicate the CP variations marked with the oval in Figure 1. During low solar activity, such variations are clearly visible. With the appearance of

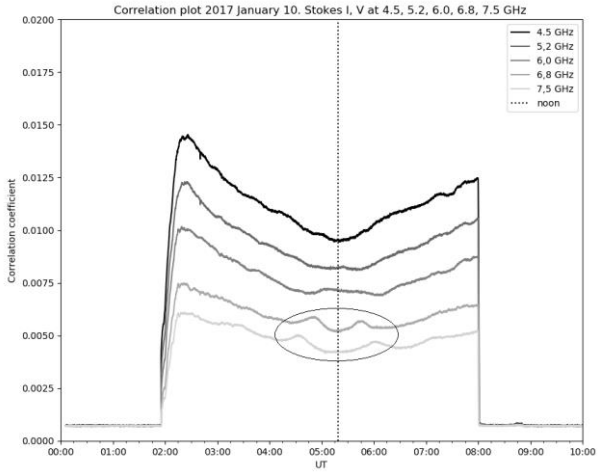

Figure 1. Correlation plot variations caused by changes in the SRH beam pattern. The oval marks variations that can be mistaken for microwave emission flux density oscillations. Diurnal CP variations are clearly visible

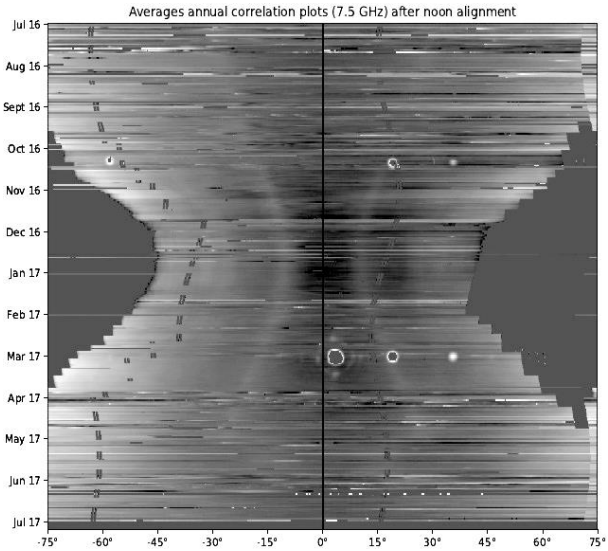

Figure 2. Correlation plots obtained from July 2016 to July 2017. Along the X-axis is the hour angle; the noon is shown by the thin solid line. Dashed black lines indicate SRH diagnostics. The light arcs symmetric about the noon denote correlation plot variations. The circles outlined by white, which are related to observation dates close to the equinox, are responses to the radiation of geostationary satellites

active regions, even in the absence of flares, the CP variations are masked by the noise of an active region. In this case, it is particularly important to suppress such variations not to confuse them with the response to the noise of the active region.

In this paper, we propose a method for simulating correlation plots as the SRH response to the quiet Sun. The simulated CPs are most similar to the real ones in the assumption that the solar limb is blurred. The essence of the method is that each CP point is calculated as the sum of a certain set of values of the solar disk visibility function. The corresponding values of this function depend on the time of observation and the SRH operating frequency. The factors influencing the result are the radius of the quiet solar disk, the degree of solar limb blur, absolute values of antenna gains, and SRH antenna shadowing.

SRH RESPONSE TO THE SOLAR DISK

SRH is a west–east–south 48 T-shaped antenna array with a spacing of 4.9 m. For imaging, we use the so-called visibilities – complex cross-correlations of signals from the antenna pairs, in which one of the antennas is in the west–east array; and the other, in the south array:

$$V'_{ij}(\nu,t)=\left\langle g_i(\nu,t)\,g_j^*(\nu,t)V_{ij}(\nu,t)\right\rangle, \quad (1)$$

where V_{ij} is the true visibility, g_i, g_j are the antenna gains in the east–west and south arrays respectively, ν is the frequency, t is the time, angle brackets denote time averaging.

To each CP point corresponds a sum of absolute values of measured visibilities of antenna pairs at a certain time at a certain frequency, i.e. a sum of absolute values of complex correlations of signals from each antenna pair

$$C(\nu,t)=\sum_{i=1}^{i=32}\sum_{j=1}^{j=16}\left|V'_{ij}(\nu,t)\right|, \quad (2)$$

where i, j are the indices of east–west and south antenna arrays respectively. The response of one antenna pair to the intensity distribution over the ξ, η angles can be written as [Thompson et al., 2003]

$$V(\nu,t)=\iint_{\Omega}F(\xi,\eta)\cos(2\pi(u\xi+\nu\eta))S(\xi,\eta)d\xi d\eta, \quad (3)$$

where $F(\xi,\eta)$ is the primary beam of SRH antennas, $S(\xi,\eta)$ is the distribution of solar emission intensity, Ω is the angular size of a source. To find the response to the solar disk, assume that the emission intensity distribution is uniform with respect to the angular diameter of the disk, and the influence of the antenna primary beam can be ignored. In this case, expression (2) will have the form

$$C(\nu,t)=\sum_{i=1}^{i=32}\sum_{j=1}^{j=16}|g_i||g_j|\times\iint_{\Omega}\cos(2\pi(u_{ij}\xi+\upsilon_{ij}\eta))d\xi d\eta=$$

$$=2\sum_{i=1}^{i=32}\sum_{j=1}^{j=16}|g_i||g_j|\times\int_{\Omega}\cos\left(2\pi\sqrt{u_{ij}^2+\upsilon_{ij}^2}\,\theta\right)\sqrt{\Omega^2/4-\theta^2}\,d\theta=$$

$$= \pi \sum_{i=1}^{i=32} \sum_{j=1}^{j=16} |g_i||g_j| \left| \frac{J_1\left(\Omega\sqrt{u_{ij}^2 + \upsilon_{ij}^2}\right)}{\Omega\sqrt{u_{ij}^2 + \upsilon_{ij}^2}} \right|, \quad (4)$$

where g_i, g_j are the i, j antenna gains; u_{ij}, υ_{ij} are the v, t-dependent spatial frequency components, J_1 is the Bessel function of the first kind, Ω is the angular size of the Sun. The numerical calculation of the model CP by expression (4) does not require operations with two-dimensional arrays, and therefore is much faster than that by expressions (2) and (3).

Figure 3 shows the sets of real (top) and simulated (bottom) complex correlations for January 10, 2018 obtained at 32 frequencies. It is clearly seen that throughout the frequency band above 6 GHz we can expect variations similar to the observed CP variations at 6.8 and 7.5 GHz (Figure 1). The CP model for the entire frequency band suggests that these temporal variations are caused by the changing response of SRH to the solar disk.

IMPACT OF ANTENNA SHADOWING ON SRH CORRELATION PLOTS

SRH is a solar dedicated instrument. This determines the required minimum distance between antennas, expressed in wavelengths – no more than the inverse of the angular diameter of the Sun. If this requirement is not met, then images are superimposed on each other just as spectra are, whose signal sampling does not satisfy the Nyquist criterion. In turn, diameters of solar radio interferometer antennas cannot be too small: this could result in the loss of sensitivity. There may therefore be situations for solar radio telescopes when one antenna of the baseline is shadowed by the adjacent antenna. The arrangement of SRH antennas is such that for negative declinations at certain times the south antenna closest to the center of the antenna array shadows adjacent east antennas at positive hour angles and the west ones at negative hour angles. The shadowing not only reduces the effective area of the corresponding two-element interferometer, but also changes its baseline with respect to the estimated baseline derived from the projection of the vector connecting antenna phase centers on the image plane. It is undesirable to exclude the shadowed antenna baselines because the largest shadowing affects the shortest baselines making the greatest contribution to the SRH response to the solar disk. Below, we examine the effect of shadowing on SRH correlation plots.

To estimate the baseline change caused by the shadowing, let us consider Figure 4. Assume that without shadowing the antenna pair baseline is determined by the distance O_1O_2. If the antenna A_1 begins to shadow A_2, the A_2 phase center will shift along the O_1O_2 line away from A_1. The magnitude of the shift can be found from the condition of equality of areas of two figures from the unshaded part of A_2 located to the left and right of the line drawn through the point O_2 normally to O_1O_2.

The area of the right figure

$$S_1(\delta) = 2\int_{\delta}^{R} \sqrt{R^2 - x^2}\, dx, \quad (5)$$

where R is the antenna half diameter. Similarly, for the area of the left figure we have

$$S_2(b, \delta) = 2\int_{-R}^{\delta} \sqrt{R^2 - x^2}\, dx - 4\int_{-R}^{-b/2} \sqrt{R^2 - x^2}\, dx. \quad (6)$$

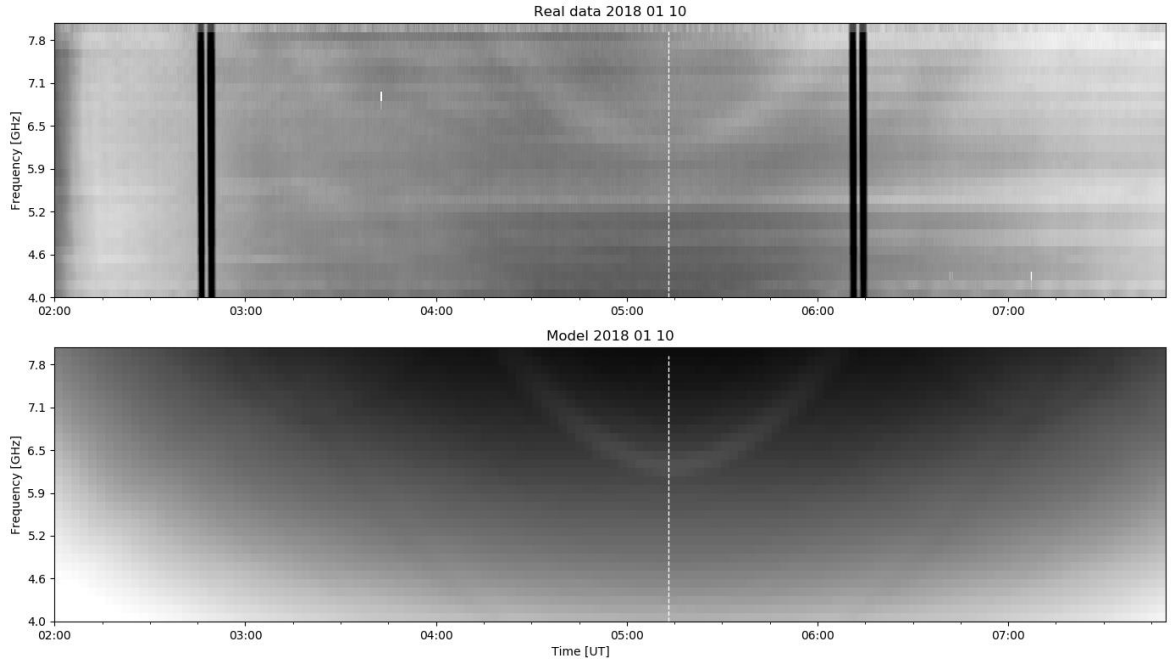

Figure 3. Correlation plots obtained at 32 frequencies in the 4–8 GHz range on January 10, 2018 (top panel): black vertical stripes indicate SRH diagnostics; the white dotted line is the noon; the correlation plot variations are particularly pronounced in the time interval 04–06 hrs at high frequencies. Model correlation plots (bottom panel) calculated in the SRH full frequency band 4–8 GHz for January 10, 2018

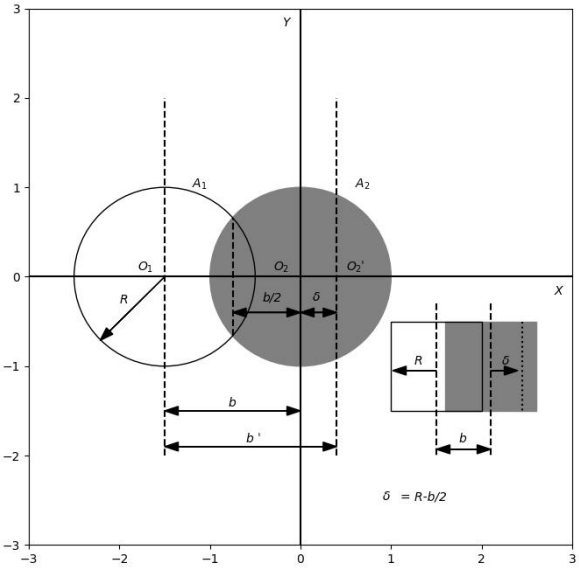

Figure 4. Schematic representation of antenna shadowing. Estimated distance between antennas *b* is the antenna baseline. If A_1 shadows A_2, the effective antenna baseline increases: $b'=b+\delta$, where δ is the gravity center of the aperture unaffected by shadowing. For the square aperture it is obvious that $\delta=R-b/2$, where *R* is the aperture half size. In the first approximation, this expression can also be used for circular apertures

The condition of equality $S_1=S_2$ yields

$$\int_0^{\delta}\sqrt{R^2-x^2}\,dx=\int_{-R}^{-b/2}\sqrt{R^2-x^2}\,dx, \qquad (7)$$

from which we can find the relationship between δ and *b*, but the expression is very cumbersome.

The result of the numerical solution of $S_1=S_2$ is presented in Figure 5. At the bottom are the δ values obtained numerically (circles) and the dependence

$$\delta=R-b/2, \qquad (8)$$

obtained in the assumption that A_1, A_2 are square apertures and shadowings occur along one of their sides (see the lower right corner of Figure 4). It is evident that such a simple expression can be used to evaluate how the antenna baseline changes due to the shadowing of one antenna by another. When shadowed, the antenna pair response with the minimum baseline will change not only due to a decrease in the collecting area, but also due to an effective increase in the baseline length. This is due to the fact that the SRH shortest antenna baseline corresponds to the vicinity of the main lobe of the solar disk visibility function. An increase in this baseline, i.e. the shift of spectral sensitivity to the region of higher spatial frequencies in the vicinity of the main lobe of the visibility function, implies a decrease in the response.

The result of the simulation of SRH correlation plots for the winter solstice is shown in Figure 6. It is seen that the shadowing exerts a significant impact by the time of observation completion and its magnitude in flux density units is no more than 1 s.f.u. at 7.5 GHz.

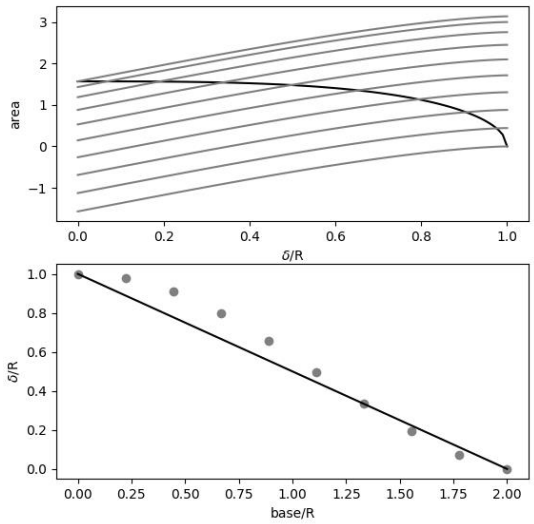

Figure 5. Result of the numerical solution of equation (7). Top panel: the black curve is S_1 (δ), the gray curves indicate S_2 (*b*, δ). Desired δ values correspond to abscissae of intersections of curves. Bottom panel: circles are the δ values found, the solid line is the δ dependence (*b*) obtained in the assumption that apertures are square. It is seen that in the first approximation we can use expression (8) to estimate the antenna baseline change caused by the shadowing

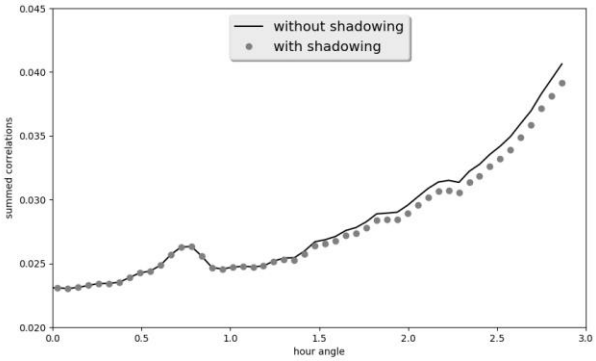

Figure 6. Correlation plot models: without regard for antenna shadowing (solid line); with regard for shadowing (–23° declination, 7.5 GHz frequency) (circles). Because of symmetry, only half of the correlation plot is shown which corresponds to positive values of the hour angle

CORRECTION OF THE SRH RESPONSE TO THE QUIET SUN

Although, as shown in Figure 3, the model correlation plots are similar to the real ones, we cannot expect an absolutely exact correspondence because the real CP is a response not only to the quiet solar disk. It is therefore possible to use at times the real CP, obtained in the absence of active regions on the solar disk, to correct the given CP.

Figure 7 shows the result of such a correction for CPs obtained on June 8–22, 2018. There were no active regions on the solar disk on June 8. The active region NOAA 12713, observed on the disk on June 15, made no significant contribution to CP, although there were weak flares. Correlation coefficients increased considerably on June 20 and 22; at that time there were many weak bursts that can be interpreted as noise of the active

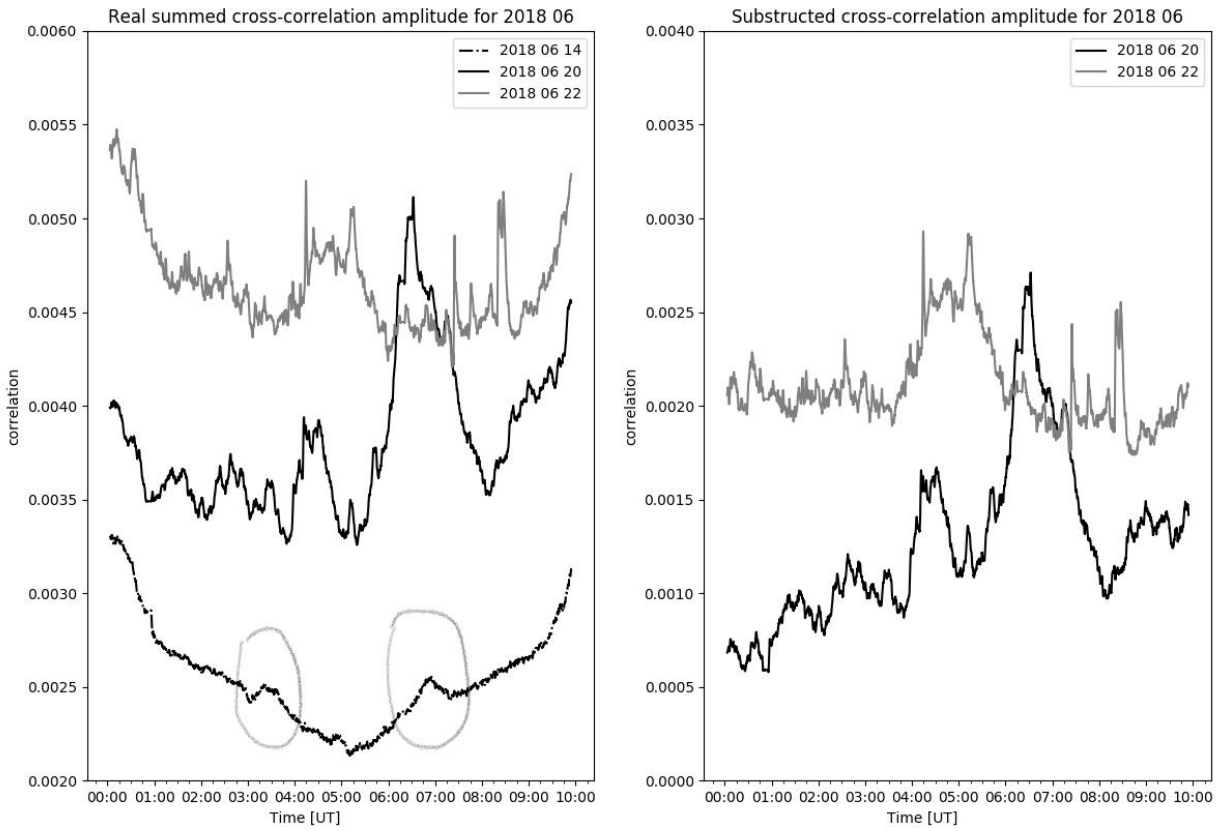

Figure 7. Correlation plots for June 14, 20, 22, 2018 (left); there was no activity on June 14; the active region NOAA12715 appeared on the disk on June 20 and 22. Ovals mark correlation plot variations caused by the response to the solar disk. The result of subtracting the correlation plot for June 8 from the plots for June 20 and 22 (right)

region, which corresponds to the moment of its emergence from under the photosphere. The result of the correction of data on June 8 is shown in the right part of the Figure. It is clearly seen that such corrected data can more accurately describe changes in the density of the emission flux from active regions, but at the same time artifacts of the correcting CP appear in the corrected CPs. In practice, this method is quite adequate if in an acceptable time interval there was no activity driven by the events of interest. The acceptability in this case is a small change in the response to the quiet Sun. In other cases, we should calculate model CPs.

Using the above method, we have computed the model CPs shown in Figure 1. We have corrected the CPs obtained at 6.8 and 7.5 GHz, where variations are most pronounced. Diurnal variations of the model and real CPs slightly differ. This is most likely due to the fact that on this day there are compact sources CPs for which vary a little during the day, so the variation of the accumulation plot is smoother than the model response to the quiet solar disk. The CP asymmetry with respect to the noon may be caused by the asymmetry in the intensity distribution over the solar disk or by the difference in gains of antennas symmetrically arranged about the center of the SRH antenna array. The most unambiguous information about antenna gains is the results of SRH diagnostics made twice a day. The diagnosis implies that all SRH antennas are pointed at the sky for some time. This enables us to estimate the difference between the responses to the sky and Sun for each antenna in the full frequency band. This difference is proportional to the absolute value of the antenna gain. To account for the remaining difference in the CP diurnal variation, it suffices to use a quadratic dependence on the hour angle in the form of $c(h)=1-(h-h_0)^2$, where $h_0$is the shift of the parabola in order to introduce the required asymmetry into the response. The correction result is shown in Figure 8. Correlation plot variations can be decreased several times, i.e. to the emission flux density level of ~0.1 s.f.u.

CONCLUSION

The proposed method for simulating SRH correlation plots describes the observed features of CPs, determined by the SRH response to the solar disk, and thus allows us to correct CPs or take into account their variations in SRH data processing. We have considered two factors affecting diurnal CP variations: SRH BP change leading to various effects of the solar disk visibility function on CPs, and the effect of antenna shadowing on antenna baselines and collecting areas. It is shown that both of these factors are most pronounced at negative solar declinations, and CP variations at high frequencies may run to 0.1 %, which corresponds to the emission flux density of 1 s.f.u. The best agreement between model CPs and real ones is obtained in the assumption that the solar limb is blurred. It is interesting to

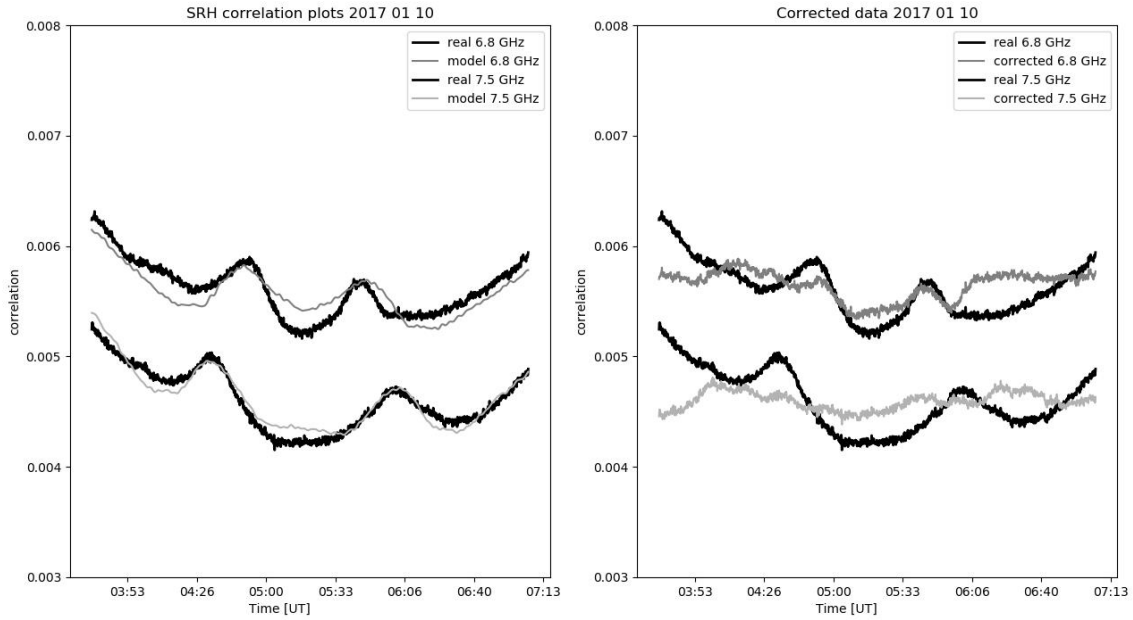

Figure 8. Result of the correction of correlation plots through model ones, calculated as a response to the solar disk (6.8 and 7.5 GHz): original plots (black curves); correction result (gray curves). The CP variations can be reduced several times to the flux density level of ~0.1 s.f.u.

shift focus of the CP simulation to the frequency dependence of the solar disk diameter and degree of solar limb blur. As for antenna shadowing, it appears that its effect is more pronounced in imaging, rather than in obtaining correlation plots. Of interest would therefore be the works on SRH BP simulation with account for antenna shadowing.

Works on Section "Effects of Mutual Antenna Shadowing on SRH Correlation Plots" were carried out using the funds of the Russian Science Foundation (project No.18-12-00172); on the other Sections, under the state task for 2018 No. 007-00163-18-00 from January 12, 2018.

REFERENCES

Grechnev V.V., Lesovoi S.V., Smolkov G.Ya., Krissinel B.B., Zandanov V.G., Altyntsev A.T., Kardapolova N.N., Sergeev R.Y., Uralov A.M., Maksimov V.P., Lubyshev B.I. The Siberian Solar Radio Telescope: the current state of the instrument, observations, and data. *Solar Phys*. 2003, vol. 216, iss. 1, pp. 239–272. DOI: 10.1023/A:1026153410061.

Knizhnik K.J., Uritsky V.M., Klimchuk J.A., DeVore C.R. Power-law statistics of driven reconnection in the magnetically closed corona. *Astrophys. J*. 2018, vol. 853, iss. 1, article id. 82, 14 p. DOI: 10.3847/1538-4357/aaa0d9.

Lesovoi S.V., Kobets V. Correlation plots of the Siberian Radioheliograph. *Solar-Terr. Phys*. 2017, vol. 3, iss. 1, pp. 19–25. DOI: 10.12737/article58f96eeb8fa318.06122835.

Lesovoi S.V., Altyntsev A.T., Ivanov E.F. Gubin A.V. The Multifrequency Siberian Radioheliograph. *Solar Phys*. 2012, vol. 280, iss. 2, pp. 651–661. DOI: 10.1007/s11207-012-0008-7.

Lesovoi S.V., Altyntsev A.T., Kochanov A.A., Grechnev V.V., Gubin A.V., Zhdanov D.A., Ivanov E.F., Uralov A.M., Kashapova L.K., Kuznetsov A.A., Meshalkina N.S., Sych R.F. Siberian Radioheliograph: first results. *Solar-Terr. Phys*. 2017, vol. 3, iss. 1, pp. 3–18. DOI: 10.12737/article_58f96ec60fec52. 86165286.

Parker E.N. Nanoflares and the solar X-ray corona. *Astrophys. J*. 1988, vol. 330, p. 474. DOI: 10.1086/166485.

Tompson A.R., Moran J.M., Svenson J.U. *Interferometriya i sintez v radioastronomii* [Interferometry and Synthesis in Radio Astronomy]. Moscow, Fizmatlit Publ., 2003. 624 p. (In Russian). English edition: Thompson A.R., Moran J.M., Swenson G.W. Interferometry and Syntnesis in Radio Astronomy: 2nd edition. Willey–VCH Publ., 2001, 715 p.

How to cite this article

Lesovoi S.V., Kobets V.S. Simulating Siberian Radioheliograph response to the quiet Sun. *Solar-Terrestrial Physics*. 2018. Vol. 4. Iss. 4. P. 82–87. DOI: 10.12737/stp-44201811.